On the Link Ergodic Capacity of MIMO MANETs using Cooperation

Renato M. de Moraes
Depart. of Computing Systems
Univ. of Pernambuco (UPE)
Recife, PE 50720-001, Brazil
Email: renato@dsc.upe.br

Hamid R. Sadjadpour
Depart. of Electrical Engineering
Univ. of California (UCSC)
Santa Cruz, CA 95064, USA
Email: hamid@soe.ucsc.edu

J.J. Garcia-Luna-Aceves
Depart. of Computer Eng. at UCSC
and Palo Alto Research Center
3333 Coyote Hill Road, Palo Alto, CA, USA
Email: jj@soe.ucsc.edu

(Invited Paper)

***Abstract*— We compute the capacity of mobile ad hoc networks (MANETs) when all the nodes in the network are endowed with M antennas. The derivation is based on a new communication scheme for wireless ad hoc networks utilizing the concept of cooperative many-to-many communication, called *opportunistic cooperation*, as opposed to the traditional approach that emphasizes on one-to-one communication. We demonstrate that the capacity of MANETs with multiple antennas is improved using cooperation as compared to non-cooperative schemes, i.e., point-to-point communication. Monte-Carlo simulation is used to validate the results.**

I. Introduction

The studies for capacity of multiple-input multiple-output (MIMO) systems concentrate on the communication between two nodes, i.e., point-to-point communication [1], [2]. The work by Jovičić et al. [5] studies the capacity of wireless ad hoc networks by assuming that the entire network is a single MIMO system in which some nodes are part of the transmitter and the remaining nodes in the network are part of the receiver, and where all the nodes have only one antenna. Their results are optimistic by assuming all the receiving nodes in the network are capable of cooperating with each other to decode the data. Furthermore, Chen and Gans [4] and Blum [3] addressed the problem of capacity for MIMO ad hoc networks assuming fading for the wireless channel. However, both works only consider small-scale fluctuations of the fading channels. Hence, Chen and Gans [4] showed that the node capacity of a MIMO ad hoc network goes to zero as the total number of nodes n increases, because all the interfering nodes have the same average power at the receiver node regardless of their distance from the receiving node.

In this paper, we include large-scale fluctuations of the channel, because, on average, adjacent interfering nodes have more destructive effects than farther nodes. We propose that a more appropriate strategy for communications among nodes in wireless ad hoc networks is a new approach based on cooperative many-to-many communication [8]. In this new paradigm, multiple nodes that are close to each other attempt to communicate concurrently. Nodes transmit and receive simultaneously using different portions of the available spectrum, which characterizes an FDMA/MIMO approach. During transmission, the node sends packets from only one of its antennas, while during reception, it uses all of its antennas to receive and decode packets from multiple nodes simultaneously. Thus, each distributed MIMO system in this scheme consists of multiple transmitting nodes acting as a single-array of multiple antennas, and a single receiver node with multiple antennas in a cell. This approach does not require any coordination among receiving nodes for decoding the received packets.

We present a tight bound on the channel capacity of MIMO MANETs when the wireless channel is modeled with both large and small-scale fluctuations. We show that per node ergodic capacity does not depend on the total number of nodes n; however, it is a function of such other network parameters as the number of receiving antennas, cell area, average node density, noise spectral density, and the path loss parameter. It is also shown that the total bandwidth required is finite for the proposed FDMA/MIMO system.

This paper is organized as follows. Section II presents the network and communication models. Section III reports the capacity analysis. Section IV shows the numerical and simulation results. We conclude the paper in section V.

II. model

A. Network Model

Consistent with prior work [6], [7], [8], we make the following sets of assumptions. There is a total of n mobile nodes in the network. Each node has an arbitrary destination to send packets and this association does not change with time. The power chosen by a node to transmit to another node is constant and equal to P. Each node transmits data to another node using a half-duplex[1] wireless link of frequency bandwidth ΔW. Also, we assume that the total area of the network grows linearly with n. The network is divided in cells. The cells have square shapes, each with area equal to a_{cell} that does not depend on n. Our model resembles the one introduced by Grossglauser and Tse [7], who consider a packet to be delivered from source to destination via one-time relaying. The position of node s at time t is indicated by $X_s(t)$. Nodes are assumed to move according to the *uniform mobility model* [7], [8], in which the steady-state distribution of the mobile nodes is uniform. Accordingly, the

This work was supported in part by CAPES/Brazil, by the US Army Research Office under grants W911NF-04-1-0224 and W911NF-05-1-0246, and by the Basking Chair of Computer Engineering.

[1] Half-duplex means that a node cannot transmit and receive data simultaneously through the same spectrum ΔW.

average node density ρ and the total network area $A_T(n)$ are related by the following definition $A_T(n) := \frac{n}{\rho}$.

Each node is assumed to know its own position (but not the position of any other node) by utilizing GPS [8], and to store a geographical map of the cells in the network with the associated frequencies as described later. The GPS receiver is also assumed to be used to provide an accurate common time reference to keep all nodes synchronized.

We use two types of channels. *Control channels* are used by nodes to obtain such information as the identities of strong interference sources, the data packets expected by destinations, and the state channel information (CSI). The detailed description of the control channel is beyond the scope of this paper but it can be found in [8]. *Data channels* are used to transmit data taking advantage of FDMA/MIMO. Each node simultaneously transmits and receives data during a communication time period, through different (non-overlapping) frequency bands (data channels). This time period of communication is called a *communication session* or simply *session*. Furthermore, each session is divided in two parts. A neighbor discovery protocol is used by nodes during the first part to obtain their neighbors information (e.g., node identifier (ID)), and the transmission of data is performed during the second part [8]. Each node has a unique ID that does not change with time.

As illustrated in Fig. 1, there are nine different cell numbers. Hence, many cells use the same number, but they are placed regularly far apart from each other to reduce interference. Thus, the frequency division assignment is such that each set of cells numbered from 1 to 9 employs different frequency channels (bandwidths). Let ξ_i denote the set of non-overlapping data frequency bands (channels) used in cell i. Accordingly, the data channels are ordered and grouped as follows. $\xi_1 = \{W_1^{(1)}, ..., W_{\mathcal{A}}^{(1)}\}$, $\xi_2 = \{W_{\mathcal{A}+1}^{(2)}, ..., W_{2\mathcal{A}}^{(2)}\}$, ..., $\xi_9 = \{W_{8\mathcal{A}+1}^{(9)}, ..., W_{9\mathcal{A}}^{(9)}\}$, in which $W_j^{(i)}$ stands for the j^{th} bandwidth in cell i, and $\mathcal{A}$ is the maximum number of nodes allowed [2] to communicate in any cell. As mentioned earlier, the signaling in the control channel provides each node in cell i knowledge of who the other nodes in the same cell are, and the node uses this information to choose a data channel to receive data in the following order based on its own ID and the IDs of its neighbors: (i) The node with the highest ID in cell i is associated (for reception) with the data channel ΔW centered at $W_{(i-1)\mathcal{A}+1}^{(i)}$ in ξ_i. (ii) The node with the second highest ID in cell i is associated (for reception) with the data channel ΔW centered at $W_{(i-1)\mathcal{A}+2}^{(i)}$ in ξ_i, and this continues for all nodes in cell i. Accordingly, the total bandwidth required for the entire network is $\Delta W_{total} = 9\mathcal{A}\Delta W$. Because ΔW and $\mathcal{A}$ are finite, the total bandwidth necessary for the FDMA/MIMO ad hoc network is also finite.

For the cell configuration given, nodes s and j in cell 5 at the center of Fig. 1 use different frequency bandwidths to communicate with each other such that, for any other node k located in another cell numbered as 5 and using the same frequency channels, it is true that $|X_k(t) - X_j(t)| \geq (1+\Delta)|X_s(t) - X_j(t)|$, where $\Delta > 0$, so that X_k is at a distance greater than $|X_s(t) - X_j(t)|$ to node j. This is called the *protocol model* and fulfills the condition for successful communication [6].

[2] The limitation on the number of nodes allowed to communicate in each cell is due to practical reasons of the MIMO systems (e.g., hardware complexity, maximum number of receive antennas, power consumption constraint, etc.).

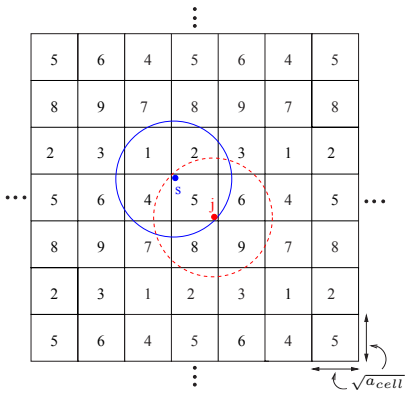

Fig. 1. Cells numbering in the network with a_{cell} as the cell area.

At time t, a cell has S nodes such that the data communication is S-to-S (see Fig. 2) where S is a random variable due to the mobility of the nodes. Each node transmits through a single antenna (employing FDMA) the same or different data packets to the other $S-1$ nodes in the same cell, using $S-1$ distinct data channels (downlink), while it simultaneously receives (through M antennas) up to $S-1$ different data packets from the other $S-1$ nodes through its assigned data channel (uplink). Hence, every node can concurrently transmits (receives) to (from) all other nodes in the same cell. Thus, multi-copies of the same packet can be simultaneously relayed to reduce delay [8].

Now, it can be shown that the fraction of cells containing $S = s$ nodes is obtained by [8]

$$\lim_{n\to\infty} \mathbb{P}\{S = s\} = \frac{1}{s!}(\rho\, a_{cell})^s e^{-\rho\, a_{cell}}. \qquad (1)$$

Consequently, the fraction of cells having more than $\mathcal{A}$ nodes can be designed to be very small, for a small positive integer $\mathcal{A}$ [8]. If a cell contains more than $\mathcal{A}$ nodes, only $\mathcal{A}$ nodes are allowed to participate in each communication session.

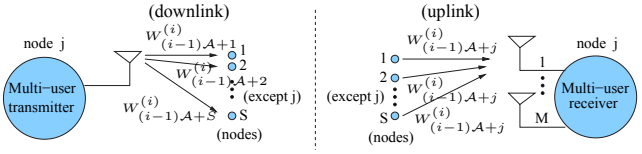

Fig. 2. FDMA/MIMO downlink and uplink description for data channels in a cell. Communication is S-to-S (i.e., many-to-many).

B. Communication Model

Without loss of generality (wolog), let the cell where node j is currently located be denoted by cell 0. Also, assume that the other cells (employing the same set of frequencies as cell 0) are numbered from $i = 1$ to ∞. P is the transmit power chosen by node s to transmit to node j. The distance between a transmitting node s (located at cell i) and the receiver j is denoted as $r_{s,j}(i)$. Assuming **no fading**, the received signal power at node j from node s is [3] $P_{s,j}(i) = P/\left(1 + r_{s,j}(i)\right)^{\alpha}$, where α is the

[3] This path loss channel model ensures that the received power is never greater than the transmitted power [5], as opposed to the common approach of $1/r_{s,j}^{\alpha}(i)$ [6], [7], [8].

path loss parameter and assumed to be greater than or equal to 2. $r_{s,j}(i)$ is not a function of receive antennas, because the distances between the transmitting node s and all M antennas of the receiver j are assumed to be equal for practical considerations.

We consider that CSI is only known at the receiver. Furthermore, as illustrated in Fig. 2, in every cell, each MIMO system consists of multiple transmitting nodes and a single receiver node (with M receiving antennas).

We use boldface capital letters to represent matrices and boldface lower case letters to denote vectors. In addition, the following standard notation will be used: $'$ for vector transpose, $\dagger$ for conjugate transpose of a matrix (or vector), $*$ for conjugate transpose of a scalar, and $\det(\cdot)$ for determinant of a matrix. Also, $\mathrm{diag}(...)$ is used to represent a diagonal matrix. The received signal vector (from cell i) for one receiver node j is defined as $\mathbf{y}_j(i) = [y_{1,j}(i), y_{2,j}(i), ..., y_{M,j}(i)]'$. The transmission vector from cell i is $\mathbf{x}(i) = [x_1(i), x_2(i), ..., x_{L_i}(i)]'$, where $L_i = \min(\mathcal{A}, S_i) - 1$ is the number of nodes in cell i transmitting in the same frequency (we assume that the nodes in cell i are transmitting in the same frequency band as that node j is using to receive data). Thus, the total transmitted power for the cell is $L_i P$ (for the frequency band in consideration). The received signal (from a cell i) for each node is defined as $\mathbf{y}_j(i) = \mathbf{H}_j(i)\,\mathbf{x}(i) + \mathbf{z}_j$, where $\mathbf{z}_j = [z_{1,j}, z_{2,j}, ..., z_{M,j}]'$ is a zero-mean complex additive white Gaussian noise (AWGN) vector. We assume that $E[\mathbf{z}_j\,\mathbf{z}_j^\dagger] = \sigma_{\mathbf{z}}^2 \mathbf{I}_M$, where $\mathbf{I}_M$ is the $M \times M$ identity matrix and $\sigma_{\mathbf{z}}^2$ is the noise variance. $\mathbf{H}_j(i)$ is the $M \times L_i$ channel matrix from cell i to node j with its elements defined as [5]

$$h_{ms,j}(i) := (\mathbf{H}_j(i))_{ms} = \frac{\phi_{ms,j}(i)}{(1+r_{s,j}(i))^{\alpha}}, \tag{2}$$

where $1 \le m \le M$, $1 \le s \le L_i$. Note that this channel modeling considers both the fading and distance effects. The fading coefficient $\phi_{ms,j}(i)$ is zero-mean, Gaussian, with independent real and imaginary parts, each with variance 1/2. Equivalently, $\phi_{ms,j}(i)$ is a stationary and ergodic stochastic fading process that is independent for each sender and receiver antenna pair, where $E_\phi[|\phi_{ms,j}(i)|^2] = 1$. $\phi_{ms,j}(i)$ can also be given in matrix notation, i.e., $\phi_{ms,j}(i) = (\mathbf{\Phi}_j(i))_{ms}$. Thus, $\mathbf{\Phi}_j(i)$ is a $M \times L_i$ matrix of complex variates whose columns are independently normally distributed with mean vector $\mathbf{0}$ and covariance matrix $\mathbf{\Psi}_j(i) = \mathbf{I}_M\, \forall(i,j)$, i.e., $N(\mathbf{0}, \mathbf{I}_M)$. Consequently, $\mathbf{\Phi}_j(i)\mathbf{\Phi}_j^\dagger(i) \sim \mathcal{W}_M(L_i, \mathbf{\Psi}_j(i))$, i.e., $\mathbf{\Phi}_j(i)\mathbf{\Phi}_j^\dagger(i)$ is a positive definite Hermitian matrix having the complex Wishart distribution [9].

III. Ergodic Capacity

Let $\mathbf{H}_j(0)$ represent the channel matrix for cell 0, i.e., $\mathbf{H}_j(0)$ describes the channel matrix to node j from the nodes in the same cell as j is located. The analysis is asymptotic in n, i.e., $n \to \infty$. Thus, $A_T(n) \to \infty$, and wolog, we consider that the cell 0 is located at the center of the network area. Given that each node transmits to another node with power P using only one antenna, and CSI is only known at the receiver side, the ergodic capacity of a receiving node j is given (in units of bits/s/Hz) by [4], [3], [2]

$$C_j = \tfrac{1}{9} E_{\mathbf{H}}\Big\{\log_2 \det\Big[\mathbf{I}_M + P\mathbf{H}_j(0)\mathbf{H}_j^\dagger(0) \cdot \Big(\sigma_{\mathbf{z}}^2\mathbf{I}_M + \textstyle\sum_{i\ge 1} P\mathbf{H}_j(i)\mathbf{H}_j^\dagger(i)\Big)^{-1}\Big]\Big\}, \tag{3}$$

where the term $\frac{1}{9}$ accounts for the frequency division multiple access, $E_{\mathbf{H}}[\cdot]$ denotes the ergodic expectation over all instantaneous $\mathbf{H}_j(i)$, and the summation in i refers to the interference coming from all cells in the network using the same frequency band ΔW as j uses for reception. Noting that $\log_2 \det(\cdot)$ is concave and using Jensen's inequality and the fact that, given j, $\mathbf{H}_j(i)$ is independent distributed for all i, we obtain

$$C_j \le \tfrac{1}{9}\log_2 \det\Big\{\mathbf{I}_M + PE_{\mathbf{H}}[\mathbf{H}_j(0)\mathbf{H}_j^\dagger(0)] \cdot E_{\mathbf{H}}\Big[\Big(\sigma_{\mathbf{z}}^2\mathbf{I}_M + P\textstyle\sum_{i\ge 1}\mathbf{H}_j(i)\mathbf{H}_j^\dagger(i)\Big)^{-1}\Big]\Big\}. \tag{4}$$

This upper bound is computed in three cases according to the transmit power level P. Compared with noise, we consider the cases of strong interference, no interference, and the intermediate case. The intermediate case is analyzed first. Accordingly, we present the following lemma.

Lemma 1 *Let the same order square Hermitian matrices* $\mathbf{G}$ *and* $\mathbf{V}$ *be positive definite. Then*

$$(\mathbf{G}+\mathbf{V})^{-1} \le \frac{1}{4}(\mathbf{G}^{-1} + \mathbf{V}^{-1}), \tag{5}$$

with equality if and only if $\mathbf{G} = \mathbf{V}$.

Proof: See Theorems 6.6 and 6.7 in [10]. ■

From (4) and Lemma 1, we obtain

$$C_j \le \tfrac{1}{9}\log_2 \det\Big\{\mathbf{I}_M + PE_{\mathbf{H}}[\mathbf{H}_j(0)\mathbf{H}_j^\dagger(0)] \cdot \Big[\tfrac{1}{4\sigma_{\mathbf{z}}^2}\mathbf{I}_M + \tfrac{1}{4P}E_{\mathbf{H}}\Big(\textstyle\sum_{i\ge 1}\mathbf{H}_j(i)\mathbf{H}_j^\dagger(i)\Big)^{-1}\Big]\Big\}. \tag{6}$$

A. Data Signal Strength Computation

Because $\mathbf{H}_j(0)$ is a $M \times L_0$ matrix with independent and identically distributed (iid) zero mean unit variance entries, then we arrive at (7) (see top of the page).

Because the distance between the transmit antenna from any other node and each receiving antenna in node j is assumed to be the same, we have

$$E_h\left[\sum_{s=1}^{L_0} h_{ms,j}(0)h_{ms,j}^*(0)\right] = E_{S,r}\left[\sum_{s=1}^{L_0}\frac{1}{(1+r_{s,j}(0))^{2\alpha}}\right], \tag{8}$$

for $1 \le m \le M$.

Therefore, we obtain

$$E_{\mathbf{H}}[\mathbf{H}_j(0)\mathbf{H}_j^\dagger(0)] = E_{S,r}\left[\sum_{s=1}^{L_0}\frac{1}{(1+r_{s,j}(0))^{2\alpha}}\right]\mathbf{I}_M. \tag{9}$$

Lemma 2 *For the uniform mobility model,*

$$E_{S,r}\left[\sum_{s=1}^{L_0}\frac{1}{(1+r_{s,j}(0))^{2\alpha}}\right] = g(a_{cell},\alpha)\,q(\mathcal{A},\rho\,a_{cell}), \tag{10}$$

where $g(a_{cell},\alpha) = \frac{4}{a_{cell}}\left[\frac{\left(1+\sqrt{\frac{a_{cell}}{2}}\right)^{2\alpha-1} - 1 - \sqrt{\frac{a_{cell}}{2}}\,(2\alpha-1)}{(2\alpha-2)(2\alpha-1)\left(1+\sqrt{\frac{a_{cell}}{2}}\right)^{2\alpha-1}}\right]$

and $q(\mathcal{A},\rho\,a_{cell}) = \sum_{S_0=2}^{\infty}\frac{[\min(\mathcal{A},S_0)-1](\rho a_{cell})^{S_0}e^{-\rho a_{cell}}}{S_0!}$.

$$E_{\mathbf{H}}[\mathbf{H}_j(0)\mathbf{H}_j^{\dagger}(0)] = \mathrm{diag}\left(E_h\left[\sum_{s=1}^{L_0} h_{1s,j}(0)h_{1s,j}^*(0)\right], E_h\left[\sum_{s=1}^{L_0} h_{2s,j}(0)h_{2s,j}^*(0)\right], \cdots, E_h\left[\sum_{s=1}^{L_0} h_{Ms,j}(0)h_{Ms,j}^*(0)\right]\right). \quad (7)$$

Proof: Because the steady state node distribution is uniform, the distances between the nodes in cell 0 and node j are iid distributed. Therefore,

$$E_{S,r}\left[\sum_{s=1}^{L_0}\frac{1}{(1+r_{s,j}(0))^{2\alpha}}\right]=\sum_{L_0=2}^{\infty} L_0\mathbb{P}\{S=S_0\}\int_0^{r_m}\frac{f_R(r)dr}{(1+r)^{2\alpha}}, \quad (11)$$

where $f_R(r)$ is the probability density function for the distance between a sender node and node j in cell 0, and r_m is their maximum distance. For a uniform node distribution and considering node j located at the center of cell 0 (for a circular cell shape), we have that [11]

$$f_R(r) = \begin{cases} \frac{2r}{r_m^2} & \text{if } 0 \le r \le r_m \\ 0 & \text{otherwise.} \end{cases} \quad (12)$$

This assumption is justified by observing that each cell in Fig. 1 can be circumvented by a circle of radius $\sqrt{\frac{a_{cell}}{2}}$. Besides, the analytical results will be contrasted with Monte-Carlo simulations for the actual ergodic capacity. Noting that the maximum possible distance inside a cell between two nodes is $r_m = \sqrt{\frac{a_{cell}}{2}}$, we obtain the following result

$$\begin{aligned}\int_0^{r_m}\frac{2rdr}{r_m^2(1+r)^{2\alpha}} &= \frac{4}{a_{cell}}\int_0^{\sqrt{\frac{a_{cell}}{2}}}\frac{rdr}{(1+r)^{2\alpha}} \\ &= \frac{4}{a_{cell}}\left[\frac{\left(1+\sqrt{\frac{a_{cell}}{2}}\right)^{2\alpha-1}-1-\sqrt{\frac{a_{cell}}{2}}(2\alpha-1)}{(2\alpha-2)(2\alpha-1)\left(1+\sqrt{\frac{a_{cell}}{2}}\right)^{2\alpha-1}}\right]. \quad (13)\end{aligned}$$

Now, from (1), the summation term in (11) becomes

$$\sum_{S_0=2}^{\infty} L_0\mathbb{P}\{S=S_0\}=\sum_{S_0=2}^{\infty}\frac{[\min(\mathcal{A},S_0)-1](\rho a_{cell})^{S_0}e^{-\rho a_{cell}}}{S_0!}. \quad (14)$$

Combining (11), (13) and (14), the final result follows. ■

B. Interference Analysis for a Tight Bound

By inspecting Fig. 1, we observe that the interfering nodes for cell 5 in the center are located in symmetry. To clarify our next approach, consider Fig. 3 which is obtained from Fig. 1, where we consider at most only the two hops away cells [12] that are interfering with the center cell (designated as cell 0). Accordingly, we can bundle the set of symmetric cells in the computation of (6) in order to obtain a tight bound, because the channel matrix associated to these interfering cells are equivalent on the average, for a uniform distribution of the nodes. Consequently, consider the following bundling and respective associated distances to receiver node j in cell 0. $\mathbf{A} = \sum_{i=1}^{4}\mathbf{\Phi}_j(i)\mathbf{\Phi}_j^{\dagger}(i)$ with $r_j(\mathbf{A}) = 3\sqrt{a_{cell}}$, $\mathbf{B} = \sum_{i=5}^{8}\mathbf{\Phi}_j(i)\mathbf{\Phi}_j^{\dagger}(i)$ with $r_j(\mathbf{B}) = 3\sqrt{2a_{cell}}$, $\mathbf{C} = \sum_{i=9}^{12}\mathbf{\Phi}_j(i)\mathbf{\Phi}_j^{\dagger}(i)$ with $r_j(\mathbf{C}) = 6\sqrt{a_{cell}}$, $\mathbf{D} = \sum_{i=13}^{20}\mathbf{\Phi}_j(i)\mathbf{\Phi}_j^{\dagger}(i)$ with $r_j(\mathbf{D}) = 3\sqrt{5a_{cell}}$, $\mathbf{E} = \sum_{i=21}^{24}\mathbf{\Phi}_j(i)\mathbf{\Phi}_j^{\dagger}(i)$ with $r_j(\mathbf{E}) = 6\sqrt{2a_{cell}}$, and consider the following lemmas.

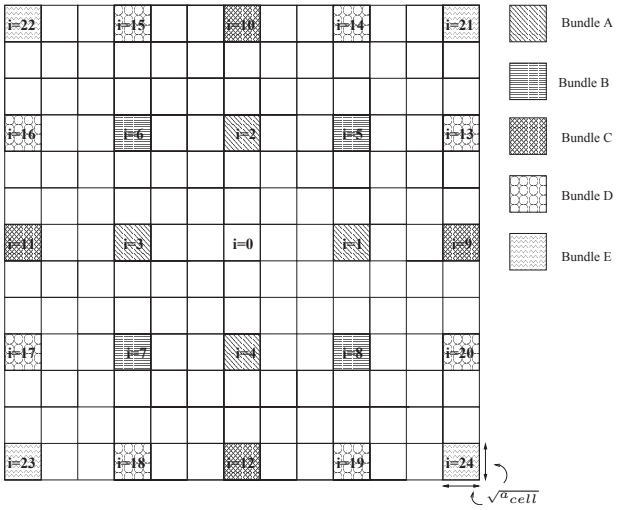

Fig. 3. Cell classification for bundling Wishart matrices.

Lemma 3 *Let $\mathbf{G}(1),...,\mathbf{G}(K)$ be independently distributed with $\mathbf{G}(i) \sim \mathcal{W}_p(q_i,\mathbf{\Psi})$ for $i = 1,...,K$. Then $\sum_{i=1}^{K}\mathbf{G}(i) \sim \mathcal{W}_p(\sum_{i=1}^{K} q_i,\mathbf{\Psi})$.*
Proof: See Theorem 3.3.8 in [13, page 94]. ■

Lemma 4 *Let $\mathbf{G}\mathbf{G}^{\dagger} \sim \mathcal{W}_p(q,\mathbf{\Psi})$. Then, for $q-p>0$*

$$E_{\mathbf{G}}[(\mathbf{G}\mathbf{G}^{\dagger})^{-1}] = \frac{1}{q-p}\mathbf{\Psi}^{-1}. \quad (15)$$

Proof: See [14]. ■

Accordingly, because the steady-state node distribution is uniform, it results that $\mathbf{A}$, $\mathbf{B}$, $\mathbf{C}$ and $\mathbf{E}$ are iid with distribution $\mathcal{W}_M(\sum_{i=1}^{4}L_i,\mathbf{I}_M)$, and $\mathbf{D} \sim \mathcal{W}_M(\sum_{i=13}^{20}L_i,\mathbf{I}_M)$. From (6), Lemma 1, 3 and 4 we obtain for two hops

$$\begin{aligned}&E_{\mathbf{H}}\left[\textstyle\sum_{i=1}^{24}\mathbf{H}_j(i)\mathbf{H}_j^{\dagger}(i)\right]^{-1} \\ &= E_{\mathbf{\Phi}}\left[\frac{\mathbf{A}}{(1+r_j(\mathbf{A}))^{2\alpha}}+\frac{\mathbf{B}}{(1+r_j(\mathbf{B}))^{2\alpha}}+\frac{\mathbf{C}}{(1+r_j(\mathbf{C}))^{2\alpha}}+\frac{\mathbf{D}}{(1+r_j(\mathbf{D}))^{2\alpha}}\right. \\ &\quad \left.+\frac{\mathbf{E}}{(1+r_j(\mathbf{E}))^{2\alpha}}\right]^{-1} \\ &\le E_{\mathbf{\Phi}}[\mathbf{D}^{-1}]\underbrace{\frac{(1+3\sqrt{5a_{cell}})^{2\alpha}}{256}}_{u_2(a_{cell},\alpha)}+E_{\mathbf{\Phi}}[\mathbf{A}^{-1}] \\ &\quad \cdot\underbrace{\left[\frac{(1+3\sqrt{a_{cell}})^{2\alpha}}{4}+\frac{(1+3\sqrt{2a_{cell}})^{2\alpha}}{16}+\frac{(1+3\sqrt{4a_{cell}})^{2\alpha}}{64}+\frac{(1+3\sqrt{8a_{cell}})^{2\alpha}}{1024}\right]}_{u_1(a_{cell},\alpha)} \\ &= u_1(a_{cell},\alpha)\sum_{S_1>\frac{M}{4}+1,\ldots,S_4>\frac{M}{4}+1}\frac{\prod_{i=1}^{4}\mathbb{P}\{S=S_i\}}{\sum_{i=1}^{4}\min(\mathcal{A},S_i)-4-M}\mathbf{I}_M \\ &\quad +u_2(a_{cell},\alpha)\sum_{S_{13}>\frac{M}{8}+1,\ldots,S_{20}>\frac{M}{8}+1}\frac{\prod_{i=13}^{20}\mathbb{P}\{S=S_i\}}{\sum_{i=13}^{20}\min(\mathcal{A},S_i)-8-M}\mathbf{I}_M \\ &:= w(\rho,a_{cell},\alpha,M,\mathcal{A})\,\mathbf{I}_M, \quad (16)\end{aligned}$$

where $\mathbb{P}\{S=S_i\}$ is given by (1) $\forall\, i$, and we used the fact that $E_{\mathbf{\Phi}}[\mathbf{A}^{-1}] = E_{\mathbf{\Phi}}[\mathbf{B}^{-1}] = E_{\mathbf{\Phi}}[\mathbf{C}^{-1}] = E_{\mathbf{\Phi}}[\mathbf{E}^{-1}]$.

We also show this by comparing our analytical results with Monte-Carlo simulation of (3) to demonstrate the tightness of capacity upper bound.

C. Capacity

The ergodic capacity of a node j follows from (6), (9), Lemma 2, and (16). Hence,

$$C_j \leq \frac{M}{9}\log_2\left[1+P\,q(\mathcal{A},\rho\,a_{cell})g(a_{cell},\alpha)\cdot\left(\frac{1}{4\sigma_{\mathbf{z}}^2}+\frac{w(\rho,a_{cell},\alpha,M,\mathcal{A})}{4P}\right)\right]. \quad (17)$$

For the case of no interference, the upper bound capacity is obtained from (4) and (10), where the term associated with interference is ignored. Accordingly, we have

$$C_j \leq \frac{M}{9}\log_2\left[1+\frac{P}{\sigma_{\mathbf{z}}^2}\,q(\mathcal{A},\rho a_{cell})g(a_{cell},\alpha)\right]. \quad (18)$$

On the other hand, if interference is strong, the term associated with noise can be neglected. Consequently, we obtain

$$C_j \leq \frac{M}{9}\log_2[1+q(\mathcal{A},\rho\,a_{cell})g(a_{cell},\alpha)w(\rho,a_{cell},\alpha,M,\mathcal{A})]\,. \quad (19)$$

Thus, from (17), (18) and (19), the node capacity grows with the number of receiving antennas M. Furthermore, because the terms in these equations do not depend on n, the node capacity does not decrease with n. Note that our channel matrix $\mathbf{H}_j(i)$ incorporates the decay with distance, i.e., $\frac{1}{(1+r_j(i))^\alpha}$, which is the large scale representation of the channel.

IV. Results

The numerical and simulation results presented here were obtained assuming that the maximum number of nodes allowed to communicate in a cell is $\mathcal{A}$ (as said in Section II-A), and considering the effect from the two hops of interference.

Fig. 4 shows the resultant node capacity upper bound indicated by the solid line as a function of the transmit power P, obtained by considering the lower-part curve from the intersection of the three curves given by (17), (18) and (19). In this figure, we also plot the Monte-Carlo simulation of (3) by averaging over 15000 random network topologies. Unlike our analytical model that interfering nodes are assumed to be located in the center of each interfering cell, the nodes are distributed randomly and uniformly in the simulation area. The result clearly shows that our upper bound obtained by bundling the Wishart matrices is close to the simulation. The intuition behind it is based on the fact that it is commonly known that the major portion of interference is caused by two adjacent hops in wireless ad hoc networks [12]. Our proposed cooperation allows nodes inside a cell to cooperate and no longer compete, by employing a distributed MIMO concept. Also, note that the adjacent interfering cells are in the same symmetric distance for any given cell. Therefore, the Wishart matrices for these channels can be bundled together which makes Lemma 1 a reasonable approach for computation of the capacity.

In addition, Fig. 4 presents the Monte-Carlo simulation for a MIMO point-to-point communication approach. In this case, we model each node using M antennas for transmission and reception. Each node uses total transmit power P. Also, in the point-to-point technique, only one pair of nodes per cell is able to communicate successfully [7]. We observe that our scheme outperforms the point-to-point case. The opportunistic cooperation is a framework that allows simultaneous many-to-many communication. Moreover, our approach is a distributed MIMO system that supports more than M transmit antennas (i.e., $\mathcal{A}-1>M$). Hence, opportunistic cooperation increases the average node capacity.

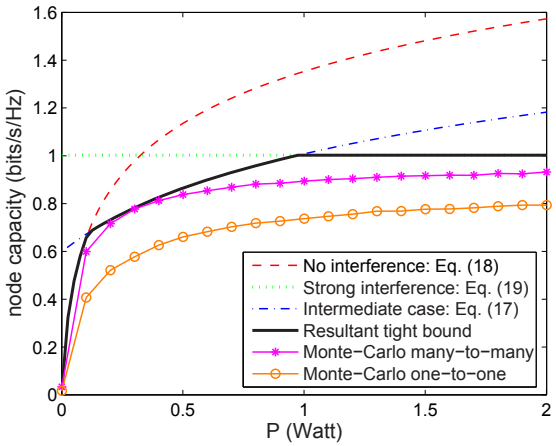

Fig. 4. Node capacity as function of power (P) for $M=2$, $a_{cell}=2m^2$, $\rho=3\,nodes/m^2$, $\sigma_{\mathbf{z}}^2=0.01$, $\alpha=2$, and $\mathcal{A}=6$.

V. Conclusions

The computation of a tight bound on the achievable capacity of MANETs with nodes having multiple antennas is an important and difficult problem. We have introduced a new cooperation scheme for such networks and computed a tight bound for the per node ergodic capacity of these networks. Our proposed opportunistic cooperation scheme demonstrates capacity improvement as compared to non-cooperative communication schemes. This capacity improvement is achieved at the expense of increase in receiver complexity for each node. The results also demonstrate that with cooperation among nodes, the capacity of the ad hoc networks increases by increasing the transmit power of the nodes for some practical values of P.

References

[1] G. J. Foschini and M. J. Gans, "On limits of wireless communications in a fading environment when using multiple antennas," *Wireless Personal Comm.*, Kluwer Academic Press, no. 6, pp. 311-355, 1998.

[2] E. Telatar, "Capacity of multi-antenna gaussian channels," *European Trans. on Telecomm.*, vol. 10, no. 6, pp. 585–595, November 1999.

[3] R. Blum, "MIMO capacity with interference," *IEEE Journal on Selected Areas in Comm.*, vol. 21, no. 5, pp. 793–801, June 2003.

[4] B. Chen and M. J. Gans, "Limiting throughput of MIMO ad hoc networks," *Proc. of IEEE International Conference on Acoustics, Speech, and Signal Processing*, Philadelphia, PA, March 2005.

[5] A. Jovičić, P. Viswanath, and S. R. Kulkarni, "Upper bounds to transport capacity of wireless networks," *IEEE Trans. on Information Theory*, vol. 50, no. 11, pp. 2555–2565, November 2004.

[6] P. Gupta and P. R. Kumar, "The capacity of wireless networks," *IEEE Trans. on Information Theory*, vol. 46, no. 2, pp. 388–404, March 2000.

[7] M. Grossglauser and D. Tse, "Mobility increases the capacity of wireless ad-hoc networks," *Proc. of IEEE Infocom*, Anchorage, AK, March 2001.

[8] R. M. de Moraes, H. R. Sadjadpour, and J. J. Garcia-Luna-Aceves, "Many-to-many communication: a new approach for collaborations in MANETs," *Proc. of IEEE Infocom*, Anchorage, AK, May 2007.

[9] A. T. James, "Distributions of matrix variates and latent roots derived from normal samples," *Annals of Mathematical Statistics*, vol. 35, no. 2, pp. 475–501, June 1964.

[10] F. Zhang, *Matrix Theory*. Springer-Verlag, 1999.

[11] C. T. Lau and C. Leung, "Capture models for mobile packet radio networks," *IEEE Trans. on Comm.*, vol. 40, no. 5, pp. 917–925, May 1992.

[12] F. Tobagi and L. Kleinrock, "Packet switching in radio channels: Part II - the hidden terminal problem in carrier sense multiple-access and the busy-tone solution," *IEEE Trans. on Comm.*, Vol. COM-23, No. 12, pp. 1417-1433, December 1975.

[13] A. K. Gupta and D. K. Nagar, *Matrix Variate Distributions*. Chapman & Hall/CRC, 2000.

[14] D. V. Rosen, "Moments for the inverted wishart distribution," *Scandinavian Journal of Statistics*, vol. 15, pp. 97–109, 1988.